Supporting Information

Synthesis, crystal structures, magnetic properties and DFT calculations of nitrate and oxalate complexes with 3,5 dimethyl-1-(2´-pyridyl)-pyrazole-Cu(II)

Pampi Pal,[†] Saugata Konar*[,‡], Mohamed Salah El Fallah[#], Kinsuk Das*[,‖], Antonio Bauzá[⊥], Antonio Frontera*[,⊥] and Subrata Mukhopadhyay[‡]

[†]*Assistant Teacher in Chemistry, Ghoshpara Nischinda Balika Vidyapith, Bally, Howrah 711227, India*

[‡]*Department of Chemistry, Jadavpur University, Jadavpur, Kolkata 700032, India. Email: saugata.konar@gmail.com*

[#]*Departament de Química Inorganica, Universitat de Barcelona, Marti I Franques, 1-11 08028 Barcelona, Catalunya, Spain*

[‖]*Department of Chemistry, Darjeeling Government College, Darjeeling 734101, India. Email: kdaschem@yahoo.in*

[⊥]*Departament de Química, Universitat de les Illes Balears, Crta. de Valldemossa km 7.5, 07122 Palma (Baleares), Spain. E-mail: toni.frontera@uib.es*

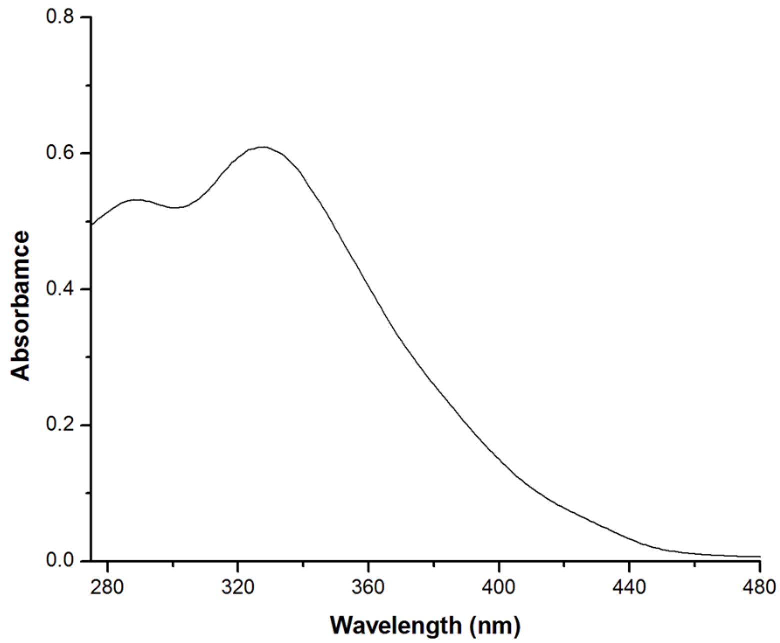

Fig. S1 UV-Vis spectrum of complex **1**

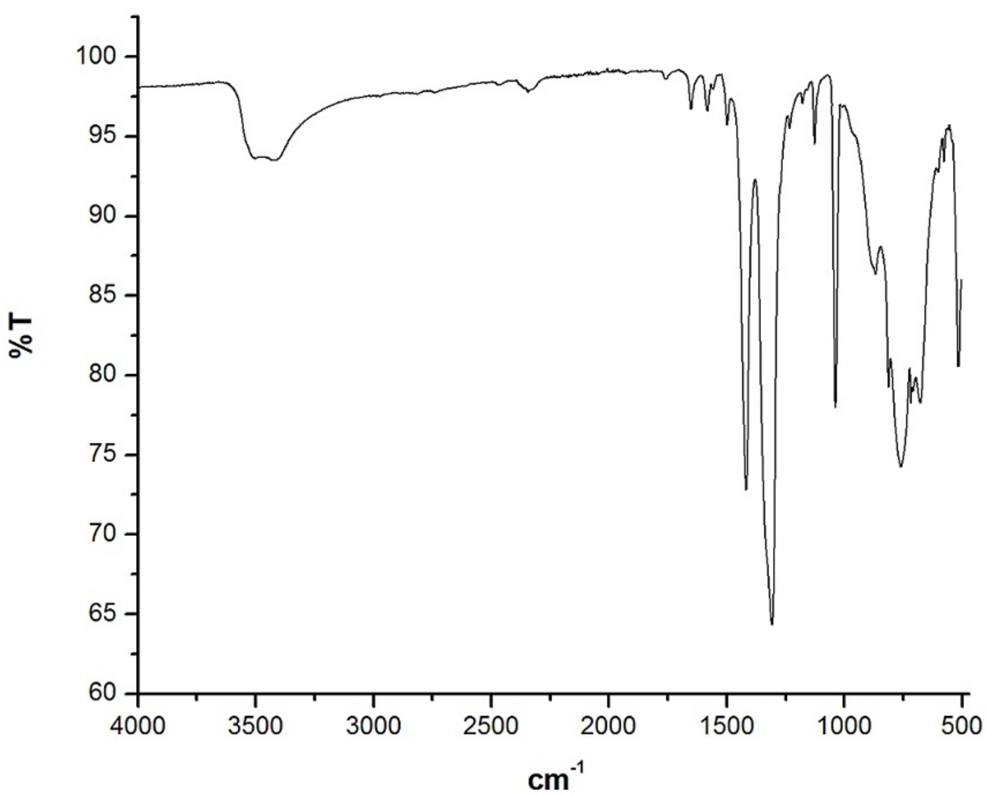

Fig. S2 IR spectrum of complex **1**

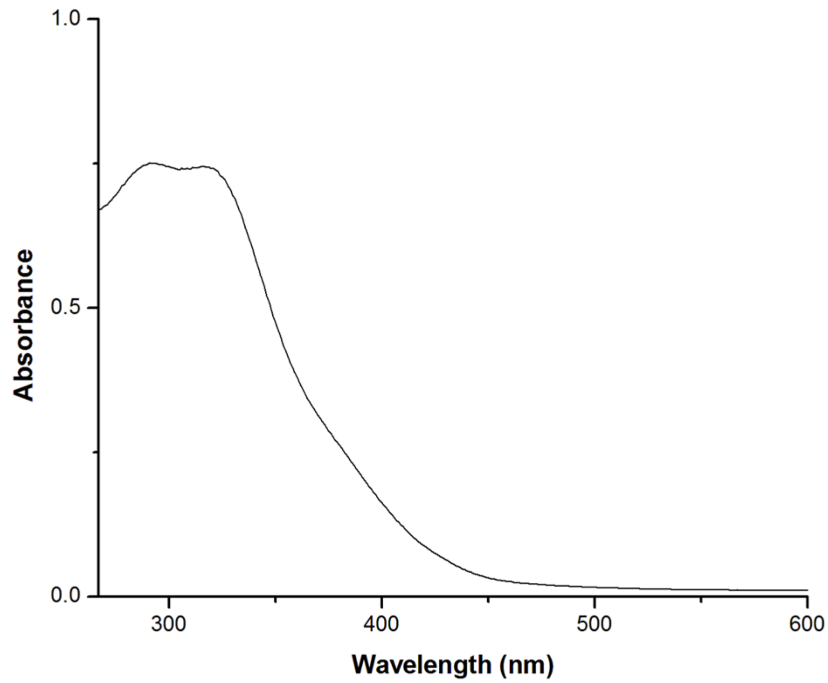

Fig. S3 UV-Vis spectrum of complex **2**

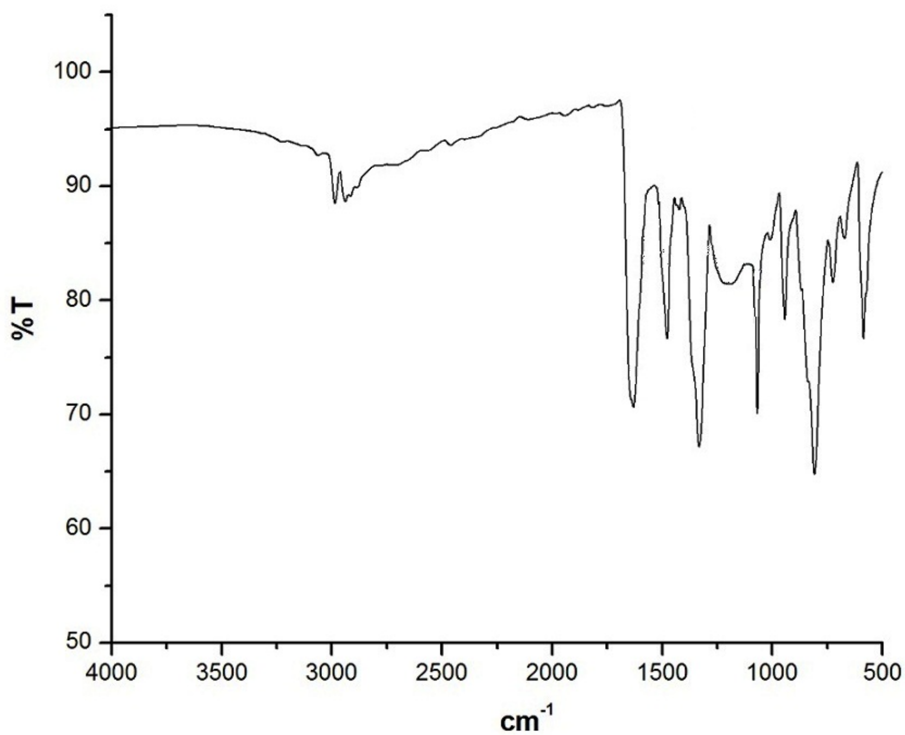

Fig. S4 IR spectrum of complex **2**

Table S1 Crystal data and structure refinement parameters for **1** and **2**

Compound	**1** (CCDC no-945288)	**2** (CCDC no-945289)
Empirical formula	$C_{10}H_{11}CuN_5O_6$	$2[C_{12}H_{11}CuN_3O_4]. H_2O$
Formula weight	360.78	667.59
Temperature (K)	90(2)	150(2)
Wavelength (Å)	0.71073	0.71073
Crystal system	Triclinic	Monoclinic
Space group	P-1	C2/c
Unit cell dimensions		
a (Å)	7.3423(3)	20.402(5)
b (Å)	8.8649(4)	7.233(5)
c (Å)	11.4482(5)	18.215(5)
α (˚)	89.440(4)	90.00
β (˚)	80.271(3)	112.363(5)
γ (˚)	67.287(3)	90.00
Volume ($Å^3$)	676.22(5)	2485.8(19)
Z	2	4
$Density_{cal}$ (Mg cm^{-3})	1.772	1.784
Absorption coefficient (mm^{-1})	2.681	1.780
F(000)	366	1360
Index ranges	$-8 \leq h \leq 8$	$-27 \leq h \leq 27$
	$-8\leq k \leq 9$	$-9 \leq k \leq 4$
	$-13\leq l \leq 13$	$-24 \leq l \leq 24$
Goodness-of-fit on F^2	1.054	1.052
Independent reflections [R_{int}]	2014 [0.032]	3077[0.024]
Absorption correction	multi-scan	multi-scan
Refinement method	Full-matrix least squares on F^2	Full-matrix least squares on F^2
Data/restraints/parameters	2014/0/201	3077/0/191
Reflections collected	4777	7801
Final R indices [I > 2σ (I)]	R=0.0477	R=0.0361
	WR2=0.1260	WR2=0.0941
Largest difference peak and hole ($eÅ^{-3}$)	-0.46, 1.01	-0.82, 0.81

Table S2 Selected bond distances (Å) and angles (°) in **1** and **2**

Bonds	Value(Å)	Angles	(°)
		Complex 1	
Cu(1)–N(1)	1.948(4)	N(1)–Cu(1)–N(3)	81.54(17)
Cu(1)–N(3)	1.977(4)	O(2)–Cu(1)–O(1)	58.05(11)
Cu(1)–O(1)	2.419(3)	O(2)–Cu(1)–N(1)	99.72(15)
Cu(1)–O(2)	1.972(3)	N(1)–Cu(1)–O(1)	113.50(13)
Cu(1)–O(5)	1.991(3)	O(2)–Cu(1)–O(5)	91.36(14)
Cu(1)–O4	2.481(3)	O(5)–Cu(1)–N(3)	92.54(15)
		O(1)–Cu(1)–N(3)	106.18(14)
		O(2)–Cu(1)–N(3)	163.47(16)
		N(1)–Cu(1)–O(5)	160.05(14)
		Complex 2	
Cu(1)–O(2)	1.951(2)	O(2)–Cu(1)–N(3)	160.89(8)
Cu(1)–O(4)	1.924(2)	O(2)–Cu(1)–O(1_a)	98.82(6)
Cu(1)–N(1)	1.988(3)	O(4)–Cu(1)–N(1)	172.05(8)
Cu(1)–N(3)	1.988(2)	O(4)–Cu(1)–N(3)	98.22(8)
Cu(1)–O(1_a)	2.284(2)	O(1_a)–Cu(1)–O(4)	102.81(2)
		N(1)–Cu(1)–N(3)	80.27(8)
		O(2)–Cu(1)–O(4)	85.18(7)
		O(2)–Cu(1)–N(1)	93.75(8)

Translation of Symmetry Code to Equiv. Pos a = [6646.00] = 3/2-x,-1/2+y, 3/2-z

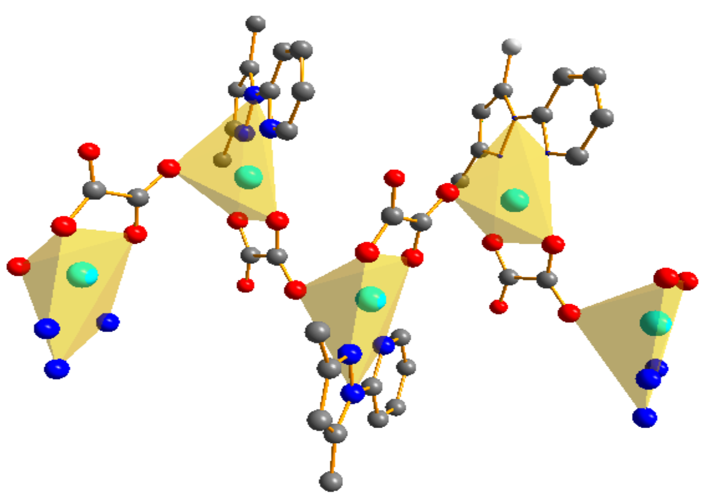

Fig. S5 1D polymeric chain along the crystallographic '*a*' axis for **2**. Hydrogen atoms are omitted for clarity. Color code: Cu(II), sky; O, red; N, blue; C, grey.

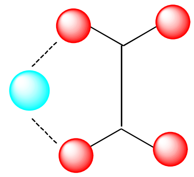	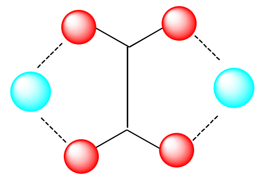	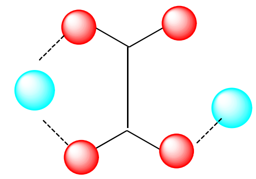
μ-oxalato κ^2O^1, O^2	μ-oxalato $1\kappa^2O^1, O^2; 2\kappa^2O^{1a}, O^{2a}$	μ-oxalato $1\kappa^2O^1, O^2; 2\kappa O^{1a}$
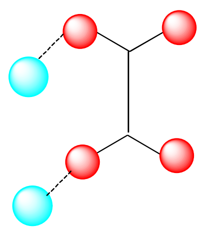	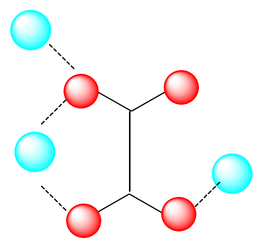	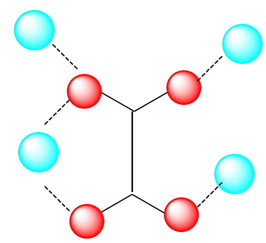
μ-oxalato $1\kappa O^1; 2\kappa O^2$	μ-oxalato $1\kappa^2O^1, O^2; 2\kappa O^1; 3\kappa O^{2a}$	μ-oxalato $1\kappa^2O^1, O^2; 2\kappa O^1;$ $3\kappa O^{1a}; 4\kappa O^{2a}$

Fig. S6 Selected binding modes of the oxalate dianion in binuclear Copper(II) complexes [‘κ’ denotes the bridging notation of oxalate dianion].

Table S3 Main structural and magnetic parameters for some oxalate bridged Cu(II) Complexes

Compound	Cu – O_{ax} (Å)	Cu – O – C (º)	Cu…..Cu (Å)	J (cm^{-1})	Ref.
$[Cu(3\text{-ampy})_2(ox)]_n$ **(3)**	2.170	111.0	5.46	-1.3	[33]
$[Cu(4\text{-ampy})_2(ox)]_n$ **(4)**	2.350	109.7	5.66	-1.1	[33]
$[Cu(en)_2][Cu(ox)_2]$ **(5)**	2.539	148.8	5.87	-1.95	[34]
$[Cu(2\text{-ampy})_2(ox)]_n$ **(6)**	2.380	107.8	5.63	+2.0	[33]
$[M(\mu\text{-ox})(isq)_2]_n$ **(7)**	2.003	117.3	5.47	+0.63	[35]
$[Cu_2(bpca)_2(ox)]$ **(8)**	2.260	107.5	5.44	+1.1	[32]
$[Cu_2(bpca)_2(H_2O)_2(ox)].2H_2O$ **(9)**	2.410	106.9	5.63	+1.0	[36]
$\{[Cu_2(L)_2(\mu\text{-ox})_2].2H_2O\}_n$ **(2)**	2.284	126.7	5.39	+1.95	**This work**
$[Cu_2(\mu\text{-ox})_2(ampy)_3]_n$ (**10**)	2.107	112.8	5.41	-22.9	[37]
$[Cu_2(L^I)_2(ox)]$ (**11**)	2.236	116.9	5.40	-12.4	[38]
$[Cu_2(DACO)_2(\mu\text{-ox})Br_2].MeOH$ (**12**)	2.016	111.4	5.24	-121	[39]
$[Cu_2(dpyam)_2(C_2O_4)(NO_3)_2((Me)_2SO)_2]$ (**13**)	1.998	112.2	5.22	-305.1	[40]

Abbreviations used: **3-ampy:** 3-aminopyridine, **4-ampy:** 4-aminopyridine, **en:** ethylene diamine, **2-ampy:** 2-aminopyridine, **isq:** isoquinoline **bpca:** bis(2-pyridylcarbonyl)amidate, **ox:** oxalate, **L:** pyridyl-pyrazole, **ampy**: 2-amino-3-methylpyridine, **L^I:** 2-N-(2'-pyridylimine) benzoic acid, **DACO:** 1,5-diazacyclooctane, **dpyam:** di-2-pyridylamine.

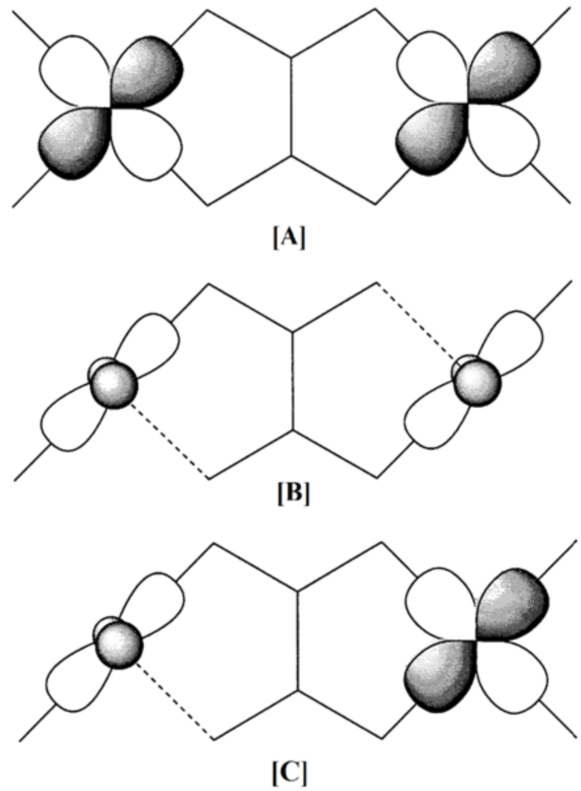

Fig. S7 Schematic representation of the orbital topologies in oxalate–copper(II) polymers

AIM analysis in complexes 1 and 2

The presence of a bond critical point (CP) and a bond path connecting two atoms is an unambiguous indication of interaction. The distribution of critical points in the dimer of compound **1** (Fig. S8) reveals the presence of a bond CP that connects the O6 with the carbon atom of the N2–C4 bond confirming the anion–π interaction. Furthermore, the distribution of CPs also reveals the presence of a bond CP connecting the O4 oxygen atom with the nitrogen atom of the pyridine ring [O···N distance is 3.347(5)]. This ancillary anion–π interaction (Fig. 7E) is likely weak because the O4 oxygen atom is coordinated to the Cu^{II} ion and the long O···N distance. In fact it can be roughly estimated as the difference between ΔE_3 and ΔE_2, which is –3.5 kcal/mol (see Fig 7, main text). Finally, the NO···NO interaction is characterized by the presence of a bond CP that connects both oxygen atoms, confirming the *pseudo* antielectrostatic interaction between the coordinate nitrate anions.

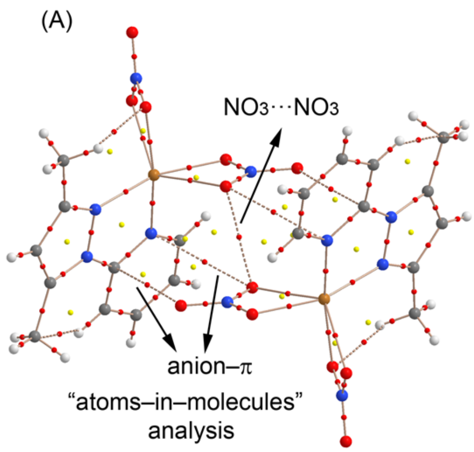

Fig. S8. AIM distribution of bond (red sphered) and ring (yellow spheres) critical points in a model dimer of compound **1**. The bond paths are also represented

For complex **2**, we have also examined the distribution of critical points of both dimeric complexes discussed in the main text (see Fig. 8 of the main text). Interestingly the distribution of critical points in the self-assembled dimer dominated by C–H/π interactions shows that, in addition to the bond CP that connects one hydrogen atom of the methyl group to the N atom of the five membered ring of the ligand, a bond CP connects two carbon atoms of the five membered rings. This additional π–π interaction revealed by the AIM analysis also explains the large interaction energy observed for this dimer (ΔE_4 = –15.0 kcal/mol) (Fig. S9 A). The distribution of CPs in the other dimer (Fig. S9 B) shows that the π–π interaction is characterized by the presence of two bond critical points that connect two carbon atoms of one pyridine ring to two the symmetrically related carbon atoms of the other pyridine ring. The interaction is further characterized by the presence of ring critical point (yellow sphere).

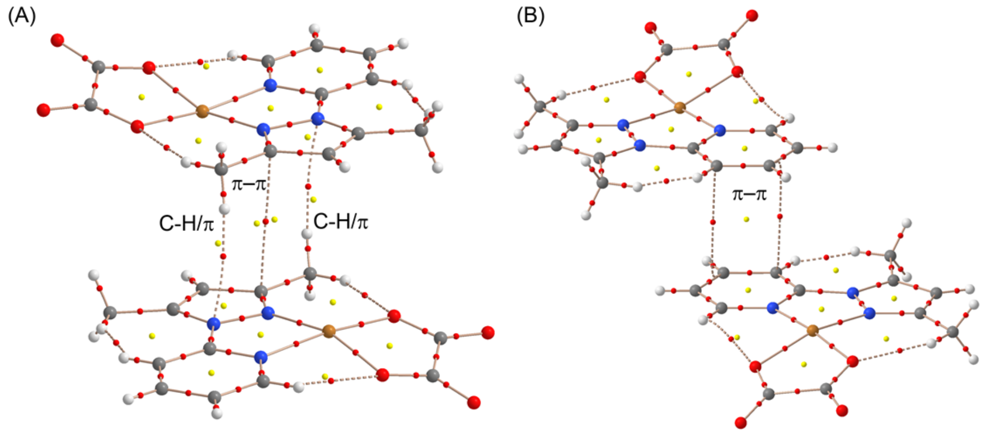

Fig. S9 AIM distribution of bond (red sphered) and ring (yellow spheres) critical points. The bond paths are also represented in the model dimers A and B of compound **2**.